

1 *Manuscript*

2 **Faster growth rates and higher mortality but similar size-**
3 **spectrum in heated, large-scale natural experiment**

4
5 Max Lindmark^{a,1}, Malin Karlsson^a, Anna Gårdmark^b

6
7 ^a Swedish University of Agricultural Sciences, Department of Aquatic Resources, Institute of
8 Coastal Research, Skolgatan 6, 742 42 Öregrund, Sweden

9
10 ^b Swedish University of Agricultural Sciences, Department of Aquatic Resources, Box 7018,
11 750 07 Uppsala, Sweden

12
13 ¹ Author to whom correspondence should be addressed. Current address:

14 Max Lindmark, Swedish University of Agricultural Sciences, Department of Aquatic
15 Resources, Institute of Marine Research, Turistgatan 5, 453 30 Lysekil, Sweden, Tel.:
16 +46(0)104784137, email: max.lindmark@slu.se

17
18
19 **Keywords:** body growth, size-structure, size-spectrum, mortality, climate change

20

21

Abstract

Ectotherms are often predicted to “shrink” with global warming. This is in line with general growth models and the temperature-size rule (TSR), both predicting smaller adult sizes with warming. However, they also predict faster juvenile growth rates, leading to larger size-at-age of young organisms. Hence, the result of warming on the size-structure of a population depends on the interplay between how mortality rate, juvenile- and adult growth rates are affected by warming. In this study, we use time series of biological samples spanning more than two decades from a unique enclosed bay heated by cooling water from a nearby nuclear power plant to become +8C warmer than its reference area. We used growth-increment biochronologies (12658 reconstructed length-at-age estimates) to quantify how >20 years of warming has affected body growth and size-at-age and catch data to quantify mortality rates and population size-structure of Eurasian perch (*Perca fluviatilis*). In the heated area, growth rates were faster for all sizes, and hence size-at-age was larger for all ages, compared to the reference area. However, mortality rates were also higher, such that the difference in the size-spectrum exponent (describing the proportion of fish by size) was relatively minor and statistically uncertain. As such, our analysis reveals that mortality, in addition to plastic growth and size-responses, is a key factor determining the size structure of populations exposed to warming. Understanding the mechanisms by which warming affects the size-structure of populations is critical for prediction the impacts of climate change on ecological functions, interactions, and dynamics.

Significance statement

Ecosystem-scale warming experiments provide unique insight into potential impacts of climate change but are very rare. Our work utilizes an experimental set-up consisting of an enclosed bay heated by cooling water from a nuclear power plant for more than two decades, and a reference area. We analyze how changes in growth and mortality have affected the size- and age distribution in a common freshwater fish using time series of catch data and growth-increment biochronologies derived from their gill lids. Despite fish in the heated area being ~10% larger at a given age, elevated mortality rates have resulted in similar size structures. Accounting for the interplay between mortality and growth is key for predicting climate impacts on the size-structure of populations.

56 Introduction

57 Ectotherm species, constituting 99% of species globally (1, 2), are commonly predicted to
58 shrink in a warming world (3–5). Mean body size responses to temperature may however be
59 uninformative, as the size-distribution of many species spans several orders of magnitude. For
60 instance, warming can shift size-distributions without altering mean size if increases in juvenile
61 size-at-age outweigh the decline in size-at-age in adults, which is consistent with the
62 temperature size-rule, TSR (6). Resolving how warming induces changes in population size-
63 distributions may thus be more instructive (7), especially for inferring warming effects on
64 species' ecological role, biomass production, or energy fluxes (8). This is because key
65 processes such as metabolism, feeding, growth, mortality scale with body size (9–14). Hence,
66 as the value of these traits at mean body size is not the same as the mean population trait value
67 (15), the size-distribution within a population matters for its dynamics and for how it changes
68 under warming.

69 The population size distribution can be represented as a size-spectrum, which generally is
70 the frequency distribution of individual body sizes (16). It is often described in terms of the
71 size-spectrum slope (slope of individuals or biomass of a size class over the mean size of that
72 class on log-log scale (16–18)) or simply the exponent of the power law individual size-
73 distribution (16). The size-spectrum thus results from temperature-dependent ecological
74 processes such as body growth, mortality and recruitment (10, 19). Despite its rich theoretical
75 foundation (20) and usefulness as an ecological indicator (21), few studies have evaluated
76 warming-effects on the species size-spectrum in larger bodied species (but see Blanchard *et*
77 *al.*(21)), and none in large scale experimental set-ups. There are numerous paths by which a
78 species' size-spectrum could change with warming (19). For instance, in line with TSR
79 predictions, warming may lead to a smaller size-spectrum exponents (steeper slope) if the
80 maximum size declines. However, changes in size-at-age and the relative abundances of

81 juveniles and adults may alter this decline in the size-spectrum slope. Warming can also lead
82 to elevated mortality (12, 22–24), which truncates the age-distribution towards younger
83 individuals (25). This may reduce density dependence and potentially increase growth rates,
84 thus countering the effects of mortality on the size spectrum exponent. However, not all sizes
85 may benefit from warming, as e.g. the optimum temperature for growth declines with size (26).
86 Hence, the effect of warming on the size-spectrum depends on several interlinked processes
87 affecting abundance-at-size and size-at-age.

88 Size-at-age is generally predicted to increase with warming for small individuals, but
89 decrease for large individuals according to the mentioned TSR (6, 27). Several factors likely
90 contribute to this pattern, such as increased allocation to reproduction (28) and larger
91 individuals in fish populations having optimum growth rates at lower temperatures (26).
92 Empirical support in fishes for this pattern seem to be more consistent for increases in size-at-
93 age of juveniles (29–31) than declines in adult size-at-age (but see (32–34)), for which a larger
94 diversity in responses is observed among species (e.g., 31, 35). However, most studies have
95 been done on commercially exploited species (since long time series are more common in such
96 species), which may confound effects of temperature plastic and/or genetic responses to size-
97 selective mortality on growth and size-at-age (36).

98 The effect of temperature on mortality rates of wild populations are more studied using
99 among-species analyses. These relationships based on thermal gradients in space may not
100 necessarily be the same as the effects of *warming* on mortality on single populations. Hence,
101 the effects of warming on growth and size-at-age and mortality within natural populations
102 constitute a key knowledge gap for predicting the consequences of climate change on
103 population size-spectra.

104 Here we used data from a unique, large-scale 23-year-long heating-experiment of a coastal
105 ecosystem to quantify how warming changed fish body growth, mortality, and the size structure

in an unexploited population of Eurasian perch (*Perca fluviatilis*, ‘perch’). We compare fish from this enclosed bay exposed to temperatures approximately 8°C above normal (‘heated area’) with fish from a reference area in the adjacent archipelago (Fig. 1). Using hierarchical Bayesian models, we quantify differences in key individual- and population level parameters, such as body growth, asymptotic size, mortality rates, and size-spectra, between the heated and reference coastal area.

Materials and Methods

Data

We use size-at-age data from perch sampled annually from an artificially heated enclosed bay (‘the Biotest basin’) and its reference area, both in the western Baltic Sea (Fig. 1). Heating started in 1980, the first analyzed cohort is 1981, and first and last catch year is 1987 and 2003, respectively, to omit transient dynamics and acute responses, and to ensure we use cohorts that only experienced one of the thermal environments during its life. A grid at the outlet of the heated area (Fig. 1) prevented fish larger than 10 cm from migrating between the areas (31, 37), and genetic studies confirm the reproductive isolation between the two populations during this time-period (38). However, the grid was removed in 2004, and since then fish growing up in the heated Biotest basin can easily swim out, fish caught in the reference area cannot be assumed to be born there. Hence, we use data only up until 2003. This resulted in 12658 length-at-age measurements from 2426 individuals in 256 net deployments.

We use data from fishing events using survey-gillnets that took place in October in the heated Biotest basin and in August in the reference area when temperatures are most comparable between the two areas (31), because temperature affect catchability in static gears. The catch was recorded by 2.5 cm length classes during 1987-2000, and into 1 cm length groups 2001-2003. To express lengths in a common length standard, 1 cm intervals were converted

into 2.5 cm intervals. The unit of catch data is hence the number of fish caught by 2.5 cm size class per net per night (i.e., a catch-per-unit-effort [CPUE] variable). All data from fishing events with disturbance affecting the catch (e.g., seal damage, strong algal growth on the gears, clogging by drifting algae) were removed (years 1996 and 1999 from the heated area in the catch data).

Length-at-age throughout life was reconstructed for a semi-random length-stratified subset of caught individuals each year. This was done using growth-increment biochronologies derived from annuli rings on the operculum bones (with control counts done on otoliths). Such analyses have become increasingly used to analyze changes in growth and size-at-age of fishes (39, 40). Specifically, an established power-law relationship between the distance of annual rings and fish length was used: $L = \kappa R^s$, where L is the length of the fish, R the operculum radius, κ the intercept, and s the slope of the line for the regression of log-fish length on log-operculum radius from a large reference data set for perch (41). Back-calculated length-at-age were obtained from the relationship $L_a = L_s (\frac{r_a}{R})^s$, where L_a is the back-calculated body length at age a , L_s is the final body length (body length at catch), r_a is the distance from the center to the annual ring corresponding to age a and $s = 0.861$ for perch (41). Since perch exhibits sexual size-dimorphism, and age-determination together with back calculation of growth was not done for males in all years, we only used females for our analyses.

Statistical Analysis

The differences in size-at-age, growth, mortality, and size structure between perch in the heated and the reference area were quantified using hierarchical linear and non-linear models fitted in a Bayesian framework. First, we describe each statistical model and then provide details of model fitting, model diagnostics and comparison.

We fit the von Bertalanffy growth equation (VBGE) (42, 43) on a log scale, describing length as a function of age to evaluate differences in size-at-age and asymptotic size: $\log(L_t) = \log(L_\infty(1 - e^{(-K(t-t_0))}))$, where L_t is the length at age (t , years), L_∞ is the asymptotic size, K is the Brody growth coefficient (yr^{-1}) and t_0 is the age when the average length was zero. We used only age- and size-at-catch as the response variables (i.e., not back-calculated length-at-age). This was to have a simpler model and not have to account for parameters varying within individuals as well as cohorts, as mean sample size per individual was only ~ 5 . We let parameters vary among cohorts rather than year of catch, because individuals within cohorts share similar environmental conditions and density dependence (39). Eight models in total were fitted (with area being dummy-coded), with different combinations of shared and area-specific parameters. We evaluated if models with area-specific parameters led to better fit and quantified the differences in area-specific parameters (indexed by subscripts heat and ref). The model with all area-specific parameter can be written as:

$$L_i \sim \text{Student-}t(v, \mu_i, \sigma) \quad (1)$$

$$\log(\mu_i) = A_{\text{ref}} \log \left[L_{\infty \text{ref}j[i]} \left(1 - e^{(-K_{\text{ref}j[i]}(t-t_{0\text{ref}j[i]}))} \right) \right] + A_{\text{heat}} \log \left[L_{\infty \text{heat}j[i]} \left(1 - e^{(-K_{\text{heat}j[i]}(t-t_{0\text{heat}j[i]}))} \right) \right] \quad (2)$$

$$\begin{bmatrix} L_{\infty \text{ref}j} \\ L_{\infty \text{heat}j} \\ K_{\text{ref}j} \\ K_{\text{heat}j} \end{bmatrix} \sim \text{MVNormal} \left(\begin{bmatrix} \mu_{L_{\infty \text{ref}}} \\ \mu_{L_{\infty \text{heat}}} \\ \mu_{K_{\text{ref}}} \\ \mu_{K_{\text{heat}}} \end{bmatrix}, \begin{bmatrix} \sigma_{L_{\infty \text{ref}}} & 0 & 0 & 0 \\ 0 & \sigma_{L_{\infty \text{heat}}} & 0 & 0 \\ 0 & 0 & \sigma_{K_{\text{ref}}} & 0 \\ 0 & 0 & 0 & \sigma_{K_{\text{heat}}} \end{bmatrix} \right) \quad (3)$$

where lengths are *Student-t* distributed to account for extreme observations, v , μ and ϕ represent the degrees of freedom, mean and the scale parameter, respectively. A_{ref} and A_{heat} are dummy variables such that $A_{\text{ref}} = 1$ and $A_{\text{heat}} = 0$ if it is the reference area, and vice versa for the heated area. The multivariate normal distribution in Eq. 3 is the prior for the cohort-varying parameters $L_{\infty \text{ref}j}$, $L_{\infty \text{heat}j}$, $K_{\text{ref}j}$ and $K_{\text{heat}j}$ (for cohorts $j = 1981, \dots, 1997$) (note that cohorts extend further back in time than the catch data), with hyper-parameters $\mu_{L_{\infty \text{ref}}}$, $\mu_{L_{\infty \text{heat}}}$,

$\mu_{K_{\text{ref}}}$, $\mu_{K_{\text{heat}}}$ describing the non-varying population means and a covariance matrix with the
 between-cohort variation along the diagonal (note we did not model a correlation between the
 parameters, hence off-diagonals are 0). The other seven models include some or all parameters
 as parameters common for the two areas, e.g., substituting $L_{\infty \text{ref}j}$ and $L_{\infty \text{heat}j}$ with $L_{\infty j}$. To aid
 convergence of this non-linear model, we used informative priors chosen after visualizing
 draws from prior predictive distributions (44) using probable parameter values (*Supporting
 Information*, Fig. S1, S7). We used the same prior distribution for each parameter class for both
 areas to not introduce any other sources of differences in parameter estimates between areas.
 We used the following priors for the VBGE model: $\mu_{L_{\infty \text{ref,heat}}} \sim N(45, 20)$,
 $\mu_{K_{\text{ref,heat}}} \sim N(0.2, 0.1)$, $t_{0 \text{ref,heat}} \sim N(-0.5, 1)$ and $v \sim \text{gamma}(2, 0.1)$. σ parameters, $\mu_{L_{\infty \text{ref}}}$,
 $\mu_{L_{\infty \text{heat}}}$, $\mu_{K_{\text{ref}}}$, $\mu_{K_{\text{heat}}}$ were given a *Student - t*(3, 0, 2.5) prior.

We also compared how body growth scales with body size (in contrast to length vs age).
 This is because size-at-age reflects lifetime growth history rather than current growth histories
 and may thus be large because growth was fast early in life, not because current growth rates
 are fast (45). We therefore fit allometric growth models describing how specific growth rate
 scales with length: $G = \alpha L^\theta$, where G , the annual specific growth between year t and $t + 1$, is
 defined as: $G = 100 \times (\log(L_{t+1}) - \log(L_t))$ and L is the geometric mean length: $L =$
 $(L_{t+1} \times L_t)^{0.5}$. Here we also used back-calculated length-at-age, resulting in multiple
 observations for each individual. As with the VBGE model, we dummy coded area to compare
 models with different combinations of common and shared parameters. We assumed growth
 rates were *Student - t* distributed, and the full model can be written as:

$$L_i \sim \text{Student} - t(v, \mu_i, \sigma) \quad (4)$$

$$\mu_i = A_{\text{ref}}(\alpha_{\text{ref}j[i], k[i]} L^{\theta_{\text{ref}}}) + A_{\text{heat}}(\alpha_{\text{heat}j[i], k[i]} L^{\theta_{\text{heat}}}) \quad (5)$$

$$\alpha_{\text{ref,heat}j} \sim N(\mu_{\alpha_{\text{ref,heat}j}}, \sigma_{\alpha_{\text{ref,heat}j}}) \quad (6)$$

$$\alpha_{\text{ref,heat}j} \sim N(\mu_{\alpha_{\text{ref,heat}j}}, \sigma_{\alpha_{\text{ref,heat}j}}) \quad (7)$$

$$\theta_{\text{ref,heat}j} \sim N(\mu_{\theta_{\text{ref,heat}j}}, \sigma_{\theta_{\text{ref,heat}j}}) \quad (8)$$

$$\theta_{\text{ref,heat}j} \sim N(\mu_{\theta_{\text{ref,heat}j}}, \sigma_{\theta_{\text{ref,heat}j}}) \quad (9)$$

We assumed only α varied across individuals j within cohorts k and compared two models: one with θ common for the heated and reference area, and one with an area-specific θ . We used the following priors, after visual exploration of the prior predictive distribution (*Supporting Information*, Fig. S8, S10): $\alpha_{\text{ref,heat}} \sim N(500, 100)$, $\theta_{\text{ref,heat}} \sim N(-1.2, 0.3)$ and $v \sim \text{gamma}(2, 0.1)$. σ , $\sigma_{\text{id:cohort}}$ and σ_{cohort} were all given a *Student - t*(3, 0, 13.3) prior.

We estimated total mortality by fitting linear models to the natural log of catch (CPUE) as a function of age (catch curve regression), under the assumption that in a closed population, the exponential decline can be described as $N_t = N_0 e^{-Zt}$, where N_t is the population at time t , N_0 is the initial population size and Z is the instantaneous mortality rate. This equation can be rewritten as a linear equation: $\log(C_t) = \log(vN_0) - Zt$, where C_t is catch at age t , if catch is assumed proportional to the number of fish (i.e., $C_t = vN_t$). Hence, the negative of the slope of the regression is the mortality rate, Z . To get catch-at-age data, we constructed area-specific age-length keys using the sub-sample of the total (female) catch that was age-determined. Age length-keys describe the age-proportions of each length-category (i.e., a matrix with length category as rows, ages as columns). Age composition is then estimated for the total catch based on the “probability” of fish in each length-category being a certain age. With fit this model with and without an $\text{age} \times \text{area}$ -interaction, and the former can be written as:

$$\log(\text{CPUE}_i) \sim \text{Student-}t(v, \mu_i, \sigma) \quad (10)$$

$$\mu_i = \beta_{0j[i]}(\text{area}_{\text{ref}}) + \beta_{1j[i]}(\text{area}_{\text{heat}}) + \beta_{2j[i]} \text{age} + \beta_{3j[i]}(\text{age} \times \text{area}_{\text{heat}}) \quad (11)$$

$$\begin{bmatrix} \beta_{0j} \\ \beta_{1j} \\ \beta_{2j} \\ \beta_{3j} \end{bmatrix} \sim \text{MVNormal} \left(\begin{bmatrix} \mu_{\beta_0} \\ \mu_{\beta_1} \\ \mu_{\beta_2} \\ \mu_{\beta_3} \end{bmatrix}, \begin{bmatrix} \sigma_{\beta_0} & 0 & 0 & 0 \\ 0 & \sigma_{\beta_1} & 0 & 0 \\ 0 & 0 & \sigma_{\beta_2} & 0 \\ 0 & 0 & 0 & \sigma_{\beta_3} \end{bmatrix} \right) \quad (12)$$

where β_{0j} and β_{1j} are the intercepts for the reference and heated areas, respectively, β_{2j} is the age slope for the reference area and β_{3j} is the interaction between *age* and *area*. All parameters vary by cohort (for cohort $j = 1981, \dots, 2000$) and their correlation is set to 0 (Eq. 12). We use the following (vague) priors: $\mu_{\beta_{0,\dots,3j}} \sim N(0, 10)$ (where μ_{β_2} is the population-level estimate for $-Z_{\text{ref}}$ and $\mu_{\beta_2} + \mu_{\beta_3}$ is the population-level estimate for $-Z_{\text{heat}}$) and $v \sim \text{gamma}(2, 0.1)$. σ and $\sigma_{\beta_{0,\dots,3}}$ were given a *Student - t*(3, 0, 2.5) prior.

Lastly, we quantified differences in the size-distributions between the areas using size-spectrum exponents. We estimate the biomass size-spectrum exponent γ directly, using the likelihood approach for binned data, i.e., the *MLEbin* method in the R package *sizeSpectra* (16, 46, 47). This method explicitly accounts for uncertainty in body masses *within* size-classes (bins) in the data and has been shown to be less biased than regression-based methods or the likelihood method based on bin-midpoints (16, 46). We pooled all years to ensure negative relationships between biomass and size in the size-classes (as the sign of the relationship varied between years).

All analyses were done using R (48) version 4.0.2 with R Studio (2021.09.1). The packages within the *tidyverse* (49) collection were used to process and visualize data. Models were fit using the R package *brms* (50). When priors were not chosen based on the prior predictive distributions, we used the default priors from *brms* as written above. We used 3 chains and 4000 iterations in total per chain. Models were compared by evaluating their expected predictive accuracy (expected log pointwise predictive density) using leave-one-out cross-validation (LOO-CV) (51) while ensuring Pareto k values < 0.7 , in the R package *loo* (52). Results of the model comparison can be found in the *Supporting Information*, Table S1-S2. We used *bayesplot* (53) and *tidybayes* (54) to process and visualize model diagnostics and posteriors. Model convergence and fit was assessed by ensuring potential scale reduction factors (\hat{R}) were less than 1.1, suggesting all three chains converged to a common distribution)

(55), and by visually inspecting trace plots, residuals QQ-plots and with posterior predictive checks (*Supporting Information*, Fig. S2, S9, S11).

Results

Analysis of fish (perch) size-at-age using the von Bertalanffy growth equation (VBGE) revealed that fish cohorts (year classes) in the heated area both grew faster initially (larger size-at-age and VBGE K parameter) and reached larger predicted asymptotic sizes than those in the unheated reference area (Fig. 2). The model with area-specific VBGE parameters (L_{∞} , K and t_0) had best out of sample predictive accuracy (the largest expected log pointwise predictive density for a new observation; Table S1), and there is a clear difference in both the estimated values for fish asymptotic length (L_{∞}) and growth rate (K) between the heated and reference area (Fig. 2B-E). For instance, the distribution of differences between the heated and reference area of the posterior samples for L_{∞} and K only had 11% and 2%, respectively, of the density below 0, illustrating that it is likely that the parameters are larger in the heated area (Fig. 2C, E). We estimated that the asymptotic length of fish in the heated area was 1.16 times larger than in the reference area ($L_{\infty\text{heat}} = 45.7[36.8, 56.3]$, $L_{\infty\text{ref}} = 39.4[35.4, 43.9]$, where the point estimate is the posterior median and values in brackets correspond to the 95% credible interval). The growth coefficient was 1.27 times larger in the heated area ($K_{\text{heat}} = 0.19[0.15, 0.23]$, $K_{\text{ref}} = 0.15[0.12, 0.17]$). Also $t_{0\text{heat}}$ was larger than $t_{0\text{ref}}$ ($-0.16[-0.21, -0.11]$ vs $-0.44[-0.56, -0.33]$, respectively). These differences in growth parameters lead to fish being approximately 10% larger in the heated area relative to the reference area (Fig. S4).

In addition, we found that growth rates in the reference area were both slower and declined faster with size compared to the heated area (Fig. 3). The best model for growth ($G = \alpha L^{\theta}$) had area-specific α and θ parameters (Table S2). Initial growth (α) was estimated to be 1.18 times

faster in the heated than in the reference area ($\alpha_{\text{heat}} = 509.7[460.1, 563.5]$, $\alpha_{\text{ref}} = 433.5[413.3, 454.1]$), and growth of fish in the heated area decline more slowly with length than in the reference area ($\theta_{\text{heat}} = -1.13[-1.16, -1.11]$, $\theta_{\text{ref}} = -1.18[-1.19, -1.16]$). The distribution of differences of the posterior samples for α and θ both only had 0.3% of the density below 0 (Fig. 3C, E), indicating high probability that length-based growth rates are faster in the heated area.

By analyzing the decline in catch-per-unit-effort over age, we found that the instantaneous mortality rate Z (rate at which log abundance declines with age) is higher in the heated area (Fig. 4). The overlap with zero is 0.05% for the distribution of differences of posterior samples of Z_{heat} and Z_{ref} (Fig. 4C). We estimated Z_{heat} to be $0.7[0.67, 0.82]$ and Z_{ref} to be $0.63[0.57, 0.68]$, which corresponds to annual mortality rates of 53% in the heated area and 47% in the reference area.

Lastly, analysis of the size-structure in the two areas revealed that, despite the faster growth rates and larger sizes in the heated area for fish of all sizes, the higher mortality rates in the heated area led to largely similar size-structures. Specifically, while largest fish were found in the heated area, the size-spectrum exponent was only slightly larger in the heated area (Fig. 5A), and their 95% confidence intervals largely overlap (Fig. 5C).

Discussion

Our study provides strong evidence for warming-induced differentiation in growth, mortality, and size-structure in a natural population of an unexploited, temperate fish species exposed to an ecosystem-scale experiment with 5-10 °C above normal temperatures for more than two decades. While it is a study on only a single species, these features make it a unique climate change experiment, as experimental studies on fish to date are much shorter and often on scales much smaller than whole ecosystems, and long time series of biological samples exist mainly

for commercially exploited fish species (29, 32, 34) (in which fisheries exploitation affects size-structure both directly and indirectly by selecting for fast growing individuals). While factors other than temperature could have contributed to the observed elevated growth and mortality, the temperature contrast is unusually large for natural systems (i.e., 5-10 °C, which can be compared to the 1.35 °C change in the Baltic Sea between 1982 and 2006 (56)). Moreover, heating occurred at the scale of a whole ecosystem, which makes the findings highly relevant in the context of global warming.

Interestingly, our findings contrast with both broader predictions about declining mean or adult body sizes based on the GOLT hypothesis (5, 57), and with intraspecific patterns such as the TSR (temperature-size rule (6)). The contrasts lie in that both asymptotic size and size-at-age of mature individuals, as well as the proportion of larger individuals were slightly larger and higher in the heated area—despite the elevated mortality rates. This result was unexpected for two reasons: optimum growth temperatures generally decline with body size within species under food satiation in experimental studies (26), and fish tend to mature at smaller body size and allocate more energy into reproduction as it gets warmer (28). Both patterns have been used to explain how growth can increase for small and young fish, while large and old fish typically do not benefit from warming. Our study species is no exception to these rules (31, 58, 59). This suggests that growth dynamics under food satiation may not be directly proportional to those under natural feeding conditions (60). Moreover, our results suggest that growth changes emerge not only from direct physiological responses to increased temperatures, but also from warming-induced changes in the food web, e.g., prey productivity, diet composition and trophic transfer efficiencies (61). It also highlights that we need to focus on understanding to what extent the commonly observed increase in size-at-age for juveniles in warm environments can be maintained as they grow older.

Our finding that mortality rates were higher in the heated area was expected—warming leads to faster metabolic rates, which in turn is associated with shorter life span (11, 62, 63) (higher “physiological” mortality). Warming may also increase predation mortality, as predators’ feeding rates increase in order to meet the higher demand of food (12, 14, 23). However, most evidence to date of the temperature dependence of mortality rates in natural populations stem from across species studies (12, 13, 64) (but see (23, 24)). Across species relationships are not necessarily determined by the same processes as within species relationships; thus, our finding of warming-induced mortality in a heated vs control environment in two nearby con-specific populations is important.

Since a key question for understanding the implications of warming on ectotherm populations is if larger individuals in a population become rarer or smaller (27, 65), within-species mortality and growth responses to warming need further study. Importantly, this requires accounting also for effects of warming on growth, and how responses in growth and mortality depend on each other. For instance, higher mortality (predation or natural, physiological mortality) can release intra-specific competition and thus increase growth. Conversely, altered growth and body sizes can lead to changes in size-specific mortality, such as predation or starvation. In conclusion, individual-level patterns such as the TSR may be of limited use for predicting changes on the population-level size structure as it does not concern changes in abundance-at-size via mortality. Mortality may, however, be an important driver of the observed shrinking of ectotherms (66). Understanding the mechanisms by which the size- and age-distribution change with warming is critical for predicting how warming changes species functions and ecological roles (7, 61, 67). Our findings demonstrate that a key to do this is to acknowledge temperature effects on both growth and mortality and how they interact.

Acknowledgements

We thank all staff involved in data collection, and Jens Olsson and Göran Sundblad for discussion. This study was supported by SLU Quantitative Fish and Fisheries Ecology.

Code and Data Availability

All data and R code to reproduce the analyses can be downloaded from a GitHub repository (https://github.com/maxlindmark/warm_life_history) and will be archived on Zenodo upon publication. Researchers interested in using the data for purposes other than replicating our analyses are advised to request the data from the authors, as other useful information from the original data might not be included.

Author Contributions

ML conceived the idea and designed the study and the statistical analysis. Data-processing, initial statistical analyses, and initial writing was done by MK and ML. AG contributed critically to all mentioned parts of the paper. All authors contributed to the manuscript writing and gave final approval for publication.

References

1. E. O. Wilson, *The Diversity of Life* (Harvard University Press, 1992).
2. D. Atkinson, R. M. Sibly, Why are organisms usually bigger in colder environments? Making sense of a life history puzzle. *Trends in Ecology & Evolution* **12**, 235–239 (1997).
3. J. L. Gardner, A. Peters, M. R. Kearney, L. Joseph, R. Heinsohn, Declining body size: a third universal response to warming? *Trends in Ecology & Evolution* **26**, 285–291 (2011).
4. J. A. Sheridan, D. Bickford, Shrinking body size as an ecological response to climate change. *Nature Climate Change* **1**, 401–406 (2011).
5. W. W. L. Cheung, *et al.*, Shrinking of fishes exacerbates impacts of global ocean changes on marine ecosystems. *Nature Climate Change* **3**, 254–258 (2013).

- 378 6. D. Atkinson, Temperature and organism size—A biological law for ectotherms?
379 *Advances in Ecological Research* **25**, 1–58 (1994).
- 380 7. K. J. Fritschie, J. D. Olden, Disentangling the influences of mean body size and size
381 structure on ecosystem functioning: an example of nutrient recycling by a non-native
382 crayfish. *Ecology and Evolution* **6**, 159–169 (2016).
- 383 8. G. Yvon-Durocher, J. M. Montoya, M. Trimmer, G. Woodward, Warming alters the size
384 spectrum and shifts the distribution of biomass in freshwater ecosystems. *Global*
385 *Change Biology* **17**, 1681–1694 (2011).
- 386 9. K. H. Andersen, Size-based theory for fisheries advice. *ICES J Mar Sci* **77**, 2445–2455
387 (2020).
- 388 10. J. L. Blanchard, R. F. Heneghan, J. D. Everett, R. Trebilco, A. J. Richardson, From
389 bacteria to whales: Using functional size spectra to model marine ecosystems. *Trends in*
390 *Ecology & Evolution* **32**, 174–186 (2017).
- 391 11. J. H. Brown, J. F. Gillooly, A. P. Allen, V. M. Savage, G. B. West, Toward a metabolic
392 theory of ecology. *Ecology* **85**, 1771–1789 (2004).
- 393 12. D. Pauly, On the interrelationships between natural mortality, growth parameters, and
394 mean environmental temperature in 175 fish stocks. *ICES Journal of Marine Science* **39**,
395 175–192 (1980).
- 396 13. J. T. Thorson, S. B. Munch, J. M. Cope, J. Gao, Predicting life history parameters for all
397 fishes worldwide. *Ecological Applications* **27**, 2262–2276 (2017).
- 398 14. E. Ursin, A Mathematical Model of Some Aspects of Fish Growth, Respiration, and
399 Mortality. *Journal of the Fisheries Research Board of Canada* **24**, 2355–2453 (1967).
- 400 15. J. R. Bernhardt, J. M. Sunday, P. L. Thompson, M. I. O'Connor, Nonlinear averaging of
401 thermal experience predicts population growth rates in a thermally variable
402 environment. *Proceedings of the Royal Society B: Biological Sciences* **285**, 20181076
403 (2018).
- 404 16. A. M. Edwards, J. P. W. Robinson, M. J. Plank, J. K. Baum, J. L. Blanchard, Testing and
405 recommending methods for fitting size spectra to data. *Methods in Ecology and*
406 *Evolution* **8**, 57–67 (2017).
- 407 17. R. W. Sheldon, W. H. Sutcliffe, A. Prakash, The Production of Particles in the Surface
408 Waters of the Ocean with Particular Reference to the Sargasso Sea1. *Limnology and*
409 *Oceanography* **18**, 719–733 (1973).
- 410 18. E. P. White, S. K. M. Ernest, A. J. Kerkhoff, B. J. Enquist, Relationships between body
411 size and abundance in ecology. *Trends in Ecology & Evolution* **22**, 323–330 (2007).
- 412 19. R. F. Heneghan, I. A. Hatton, E. D. Galbraith, Climate change impacts on marine
413 ecosystems through the lens of the size spectrum. *Emerging Topics in Life Sciences* **3**,
414 233–243 (2019).

- 415 20. K. H. Andersen, *Fish Ecology, Evolution, and Exploitation: A New Theoretical Synthesis*
416 (Princeton University Press, 2019).
- 417 21. J. L. Blanchard, *et al.*, Do climate and fishing influence size-based indicators of Celtic
418 Sea fish community structure? *ICES Journal of Marine Science* **62**, 405–411 (2005).
- 419 22. H. K. Barnett, T. P. Quinn, M. Bhuthimethee, J. R. Winton, Increased prespawning
420 mortality threatens an integrated natural- and hatchery-origin sockeye salmon
421 population in the Lake Washington Basin. *Fisheries Research* **227**, 105527 (2020).
- 422 23. P. A. Biro, J. R. Post, D. J. Booth, Mechanisms for climate-induced mortality of fish
423 populations in whole-lake experiments. *Proceedings of the National Academy of*
424 *Sciences* **104**, 9715–9719 (2007).
- 425 24. T. Berggren, U. Bergström, G. Sundblad, Ö. Östman, Warmer water increases early body
426 growth of northern pike (*Esox lucius*) but mortality has larger impact on decreasing
427 body sizes. *Can. J. Fish. Aquat. Sci.* (2021) <https://doi.org/10.1139/cjfas-2020-0386>
428 (October 27, 2021).
- 429 25. L. A. K. Barnett, T. A. Branch, R. A. Ranasinghe, T. E. Essington, Old-Growth Fishes
430 Become Scarce under Fishing. *Current Biology* **27**, 2843–2848.e2 (2017).
- 431 26. M. Lindmark, J. Ohlberger, A. Gårdmark, Optimum growth temperature declines with
432 body size within fish species. *Global Change Biology* **28**, 2259–2271 (2022).
- 433 27. J. Ohlberger, Climate warming and ectotherm body size – from individual physiology to
434 community ecology. *Functional Ecology* **27**, 991–1001 (2013).
- 435 28. H. F. Wootton, J. R. Morrongiello, T. Schmitt, A. Audzijonyte, Smaller adult fish size in
436 warmer water is not explained by elevated metabolism. *Ecology Letters* **25**, 1177–1188
437 (2022).
- 438 29. R. E. Thresher, J. A. Koslow, A. K. Morison, D. C. Smith, Depth-mediated reversal of
439 the effects of climate change on long-term growth rates of exploited marine fish.
440 *Proceedings of the National Academy of Sciences, USA* **104**, 7461–7465 (2007).
- 441 30. A. Rindorf, H. Jensen, C. Schrum, Growth, temperature, and density relationships of
442 North Sea cod (*Gadus morhua*). *Canadian Journal of Fisheries and Aquatic Sciences*
443 **65**, 456–470 (2008).
- 444 31. M. Huss, M. Lindmark, P. Jacobson, R. M. van Dorst, A. Gårdmark, Experimental
445 evidence of gradual size-dependent shifts in body size and growth of fish in response to
446 warming. *Glob Change Biol* **25**, 2285–2295 (2019).
- 447 32. S. Smoliński, *et al.*, Century-long cod otolith biochronology reveals individual growth
448 plasticity in response to temperature. *Sci Rep* **10**, 16708 (2020).
- 449 33. K. B. Oke, F. J. Mueter, M. A. Litzow, Warming leads to opposite patterns in weight-at-
450 age for young versus old age classes of Bering Sea walleye pollock. *Can. J. Fish. Aquat.*
451 *Sci.* (2022) <https://doi.org/10.1139/cjfas-2021-0315> (July 22, 2022).

- 452 34. A. R. Baudron, C. L. Needle, A. D. Rijnsdorp, C. T. Marshall, Warming temperatures
453 and smaller body sizes: synchronous changes in growth of North Sea fishes. *Global*
454 *Change Biology* **20**, 1023–1031 (2014).
- 455 35. D. R. Barneche, M. Jahn, F. Seebacher, Warming increases the cost of growth in a model
456 vertebrate. *Functional Ecology* **33**, 1256–1266 (2019).
- 457 36. A. Audzijonyte, *et al.*, Trends and management implications of human-influenced life-
458 history changes in marine ectotherms. *Fish and Fisheries* **17**, 1005–1028 (2016).
- 459 37. A. Adill, K. Mo, A. Sevastik, J. Olsson, L. Bergström, “Biologisk recipientkontroll vid
460 Forsmarks kärnkraftverk (in Swedish)” (2013) (August 10, 2021).
- 461 38. M. Björklund, T. Aho, J. Behrmann-Godel, Isolation over 35 years in a heated biotest
462 basin causes selection on MHC class II β genes in the European perch (*Perca fluviatilis*
463 L.). *Ecol Evol* **5**, 1440–1455 (2015).
- 464 39. J. R. Morrongiello, R. E. Thresher, A statistical framework to explore ontogenetic growth
465 variation among individuals and populations: a marine fish example. *Ecological*
466 *Monographs* **85**, 93–115 (2015).
- 467 40. T. E. Essington, M. E. Matta, B. A. Black, T. E. Helser, P. D. Spencer, Fitting growth
468 models to otolith increments to reveal time-varying growth. *Can. J. Fish. Aquat. Sci.* **79**,
469 159–167 (2022).
- 470 41. G. Thoreson, “Metoder för övervakning av kustfiskbestånd (in Swedish)”
471 (Kustlaboratoriet, Fiskeriverket, 1996) (September 28, 2021).
- 472 42. R. J. H. Beverton, S. J. Holt, *On the Dynamics of Exploited Fish Populations* (Fishery
473 Investigations London Series 2, Volume 19., 1957).
- 474 43. L. von Bertalanffy, A quantitative theory of organic growth (inquiries on growth laws.
475 II). *Human Biology* **10**, 181–213 (1938).
- 476 44. J. S. Wesner, J. P. F. Pomeranz, Choosing priors in Bayesian ecological models by
477 simulating from the prior predictive distribution. *Ecosphere* **12**, e03739 (2021).
- 478 45. K. Lorenzen, Toward a new paradigm for growth modeling in fisheries stock
479 assessments: Embracing plasticity and its consequences. *Fisheries Research* **180**, 4–22
480 (2016).
- 481 46. A. M. Edwards, J. P. W. Robinson, J. L. Blanchard, J. K. Baum, M. J. Plank, Accounting
482 for the bin structure of data removes bias when fitting size spectra. *Marine Ecology*
483 *Progress Series* **636**, 19–33 (2020).
- 484 47. A. Edwards, sizeSpectra: Fitting Size Spectra to Ecological Data Using Maximum
485 Likelihood (2020).
- 486 48. R Core Team, *R: A Language and Environment for Statistical Computing*. R Foundation
487 for Statistical Computing (2020).

- 488 49. H. Wickham, *et al.*, Welcome to the tidyverse. *Journal of Open Source Software*, 1686
489 (2019).
- 490 50. P.-C. Bürkner, **brms** : An R Package for Bayesian Multilevel Models Using Stan. *Journal*
491 *of Statistical Software* **80** (2017).
- 492 51. A. Vehtari, A. Gelman, J. Gabry, Practical Bayesian model evaluation using leave-one-
493 out cross-validation and WAIC. *Stat Comput* **27**, 1413–1432 (2017).
- 494 52. A. Vehtari, *et al.*, loo: Efficient leave-one-out cross-validation and WAIC for Bayesian
495 models. (2020).
- 496 53. J. Gabry, D. Simpson, A. Vehtari, M. Betancourt, A. Gelman, Visualization in Bayesian
497 workflow. *J. R. Stat. Soc. A* **182**, 389–402 (2019).
- 498 54. M. Kay, tidybayes: Tidy Data and Geoms for Bayesian Models (2019).
- 499 55. A. Gelman, J. Carlin, H. Stern, D. Rubin, *Bayesian Data Analysis. 2nd edition* (Chapman
500 and Hall/CRC, 2003).
- 501 56. I. M. Belkin, Rapid warming of large marine ecosystems. *Progress in Oceanography* **81**,
502 207–213 (2009).
- 503 57. D. Pauly, The gill-oxygen limitation theory (GOLT) and its critics. *Science Advances* **7**,
504 eabc6050 (2021).
- 505 58. P. Karås, G. Thoreson, An application of a bioenergetics model to Eurasian perch (*Perca*
506 *fluviatilis* L.). *Journal of Fish Biology* **41**, 217–230 (1992).
- 507 59. O. Sandström, E. Neuman, G. Thoreson, Effects of temperature on life history variables
508 in perch. *Journal of Fish Biology* **47**, 652–670 (1995).
- 509 60. S. F. Railsback, What We Don't Know About the Effects of Temperature on Salmonid
510 Growth. *Transactions of the American Fisheries Society* **151**, 3–12 (2022).
- 511 61. A. Gårdmark, M. Huss, Individual variation and interactions explain food web responses
512 to global warming. *Philosophical Transactions of the Royal Society B: Biological*
513 *Sciences* **375**, 20190449 (2020).
- 514 62. M. W. McCoy, J. F. Gillooly, Predicting natural mortality rates of plants and animals.
515 *Ecology Letters* **11**, 710–716 (2008).
- 516 63. S. B. Munch, S. Salinas, Latitudinal variation in lifespan within species is explained by
517 the metabolic theory of ecology. *Proceedings of the National Academy of Sciences* **106**,
518 13860–13864 (2009).
- 519 64. H. Gislason, N. Daan, J. C. Rice, J. G. Pope, Size, growth, temperature and the natural
520 mortality of marine fish: Natural mortality and size. *Fish and Fisheries* **11**, 149–158
521 (2010).
- 522 65. J. Ohlberger, E. J. Ward, D. E. Schindler, B. Lewis, Demographic changes in Chinook
523 salmon across the Northeast Pacific Ocean. *Fish and Fisheries* **19**, 533–546 (2018).

- 524 66. I. Peralta-Maraver, E. L. Rezende, Heat tolerance in ectotherms scales predictably with
525 body size. *Nat. Clim. Chang.* **11**, 58–63 (2021).
- 526 67. A. Audzijonyte, *et al.*, Fish body sizes change with temperature but not all species shrink
527 with warming. *Nat Ecol Evol* **4**, 809–814 (2020).

528

529

530

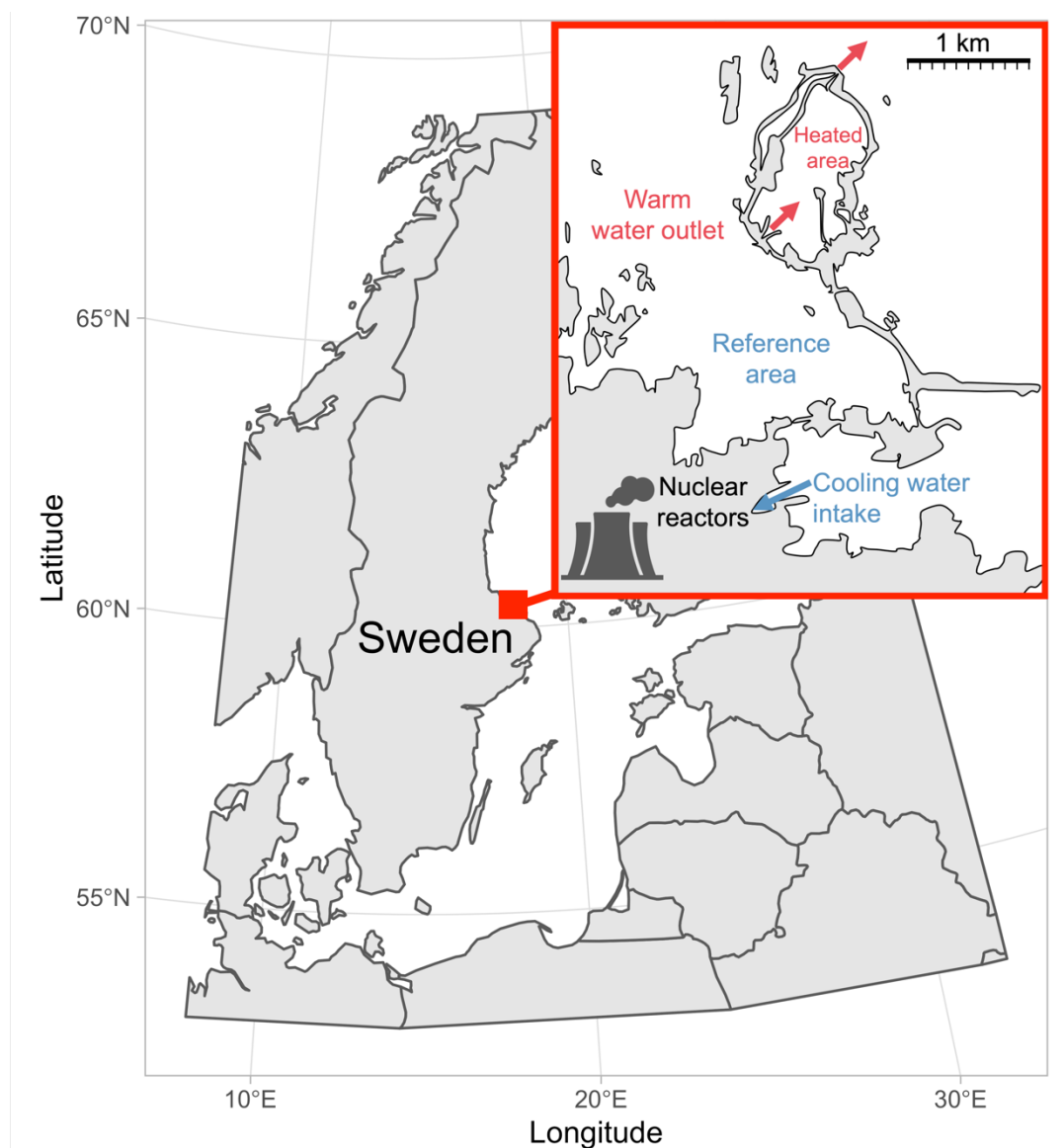


Fig. 1. Map of the area with the unique whole-ecosystem warming experiment from which perch in this study was sampled. Inset shows the 1 km² enclosed coastal bay that has been artificially heated for 23 years, the adjacent reference area with natural temperatures, and locations of the cooling water intake and where the heated water outlet from nuclear power plants enters the heated coastal basin.

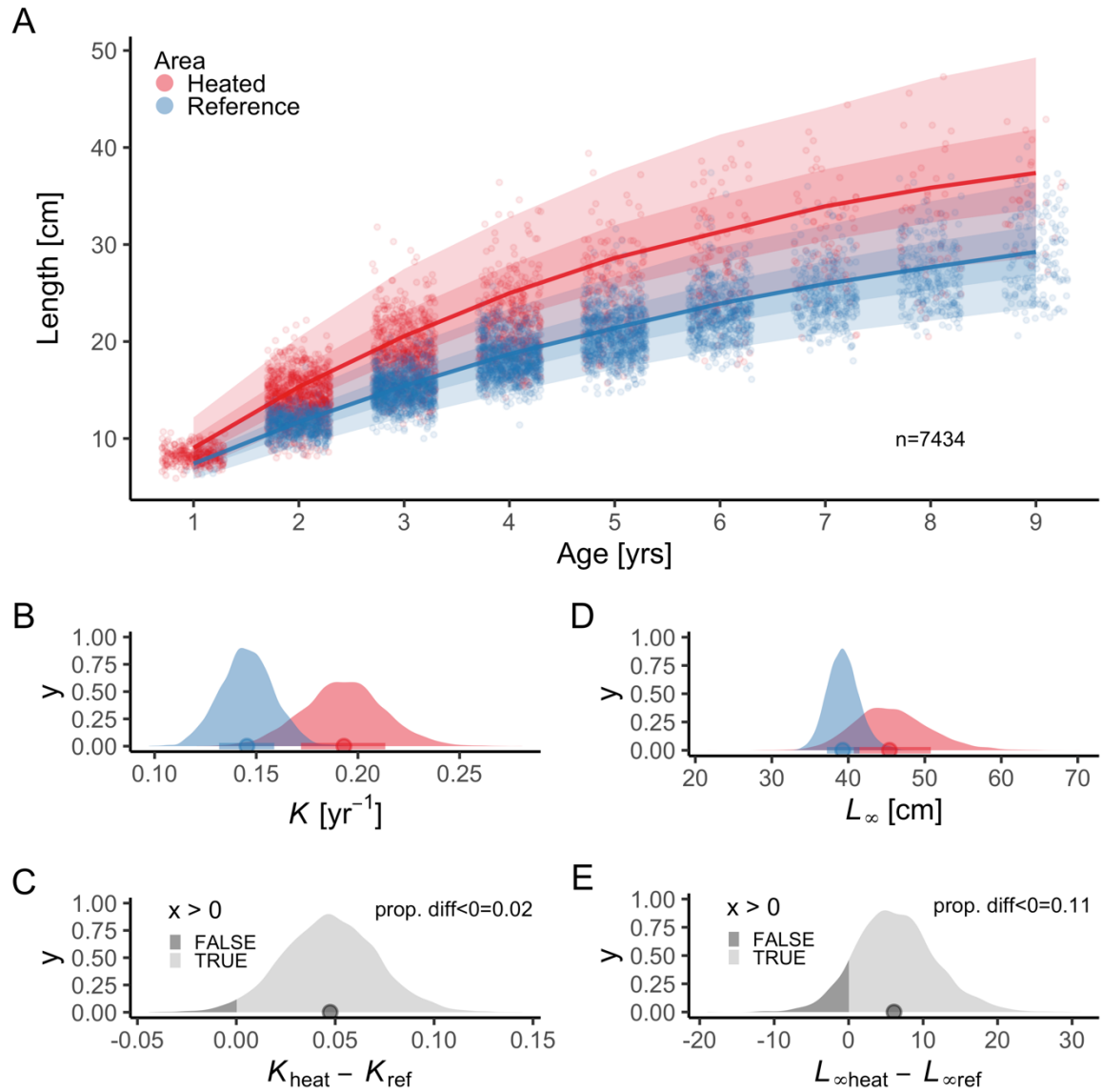


Fig. 2. Fish grow faster and reach larger sizes in the heated (red) enclosed bay compared to the reference (blue) area. Points in panel (A) depict individual-level length-at-age and lines show the global posterior prediction (both exponentiated) without group-level effects (i.e., cohort) from the von Bertalanffy growth model with area-specific coefficients. The shaded areas correspond to 50% and 90% credible intervals. Panel (B) shows the posterior distributions for growth coefficient (parameters K_{heat} (red) and K_{ref} (blue)) and (C) the distribution of their difference. Panel (D) shows the posterior distributions for asymptotic length (parameters $L_{\infty\text{heat}}$ and $L_{\infty\text{ref}}$), and (E) the distribution of their difference.

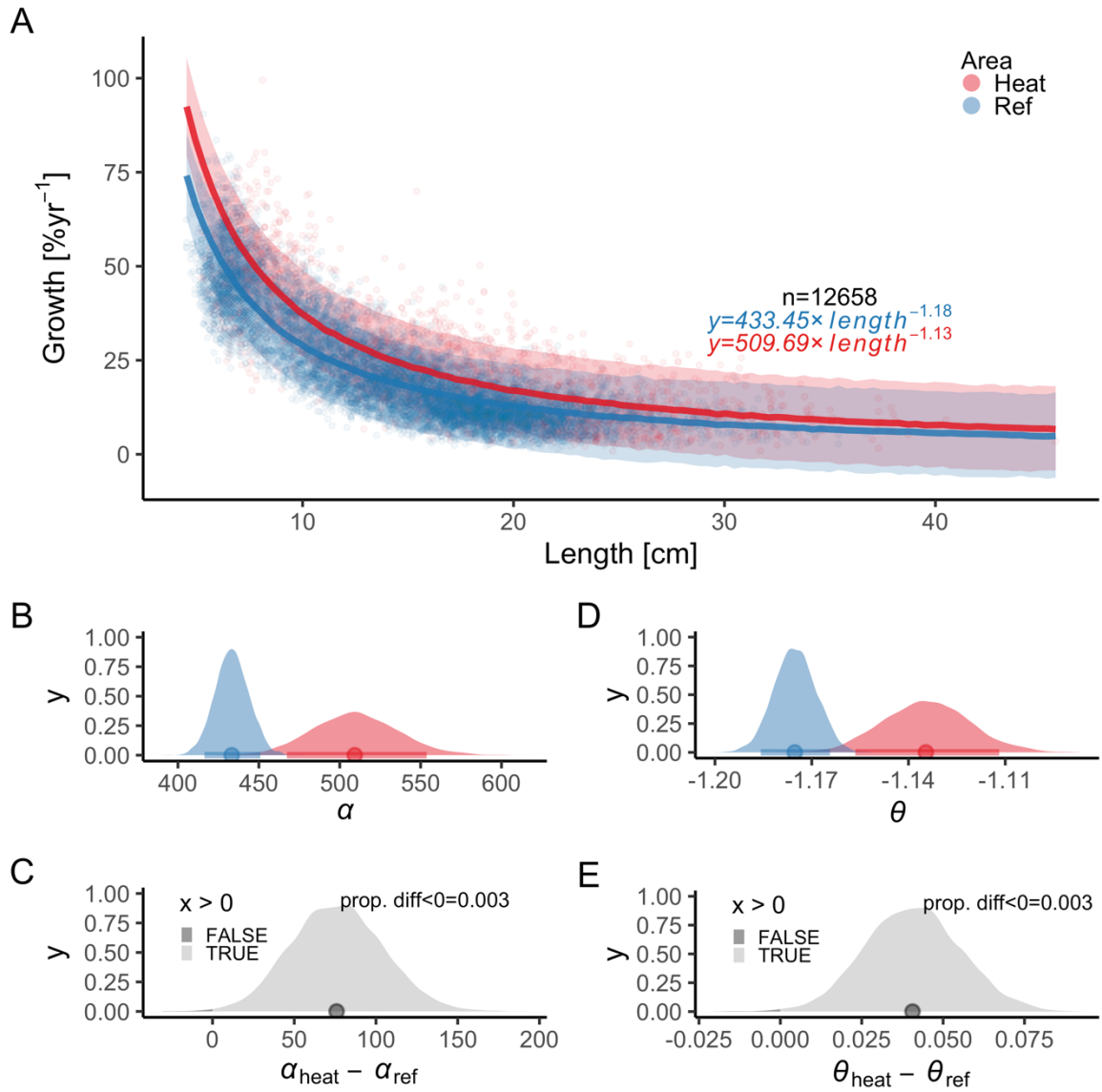


Fig. 3. The faster growth rates in the heated area (red) compared to the reference (blue) are maintained as fish grow. The points illustrate specific growth estimated from back-calculated length-at-age (within individuals) as a function of length (expressed as the geometric mean of the length at the start and end of the time interval). Lines show the global posterior prediction without group-level effects (i.e., individual within cohort) from the allometric growth model with area-specific coefficients. The shaded areas correspond to the 90% credible interval. The equation uses mean parameter estimates. Panel (B) shows the posterior distributions for initial growth (α_{heat} (red) and α_{ref} (blue)), and (C) the distribution of their difference. Panel (D) shows the posterior distributions for the allometric decline in growth with length (θ_{heat} and θ_{ref}), and (E) the distribution of their difference.

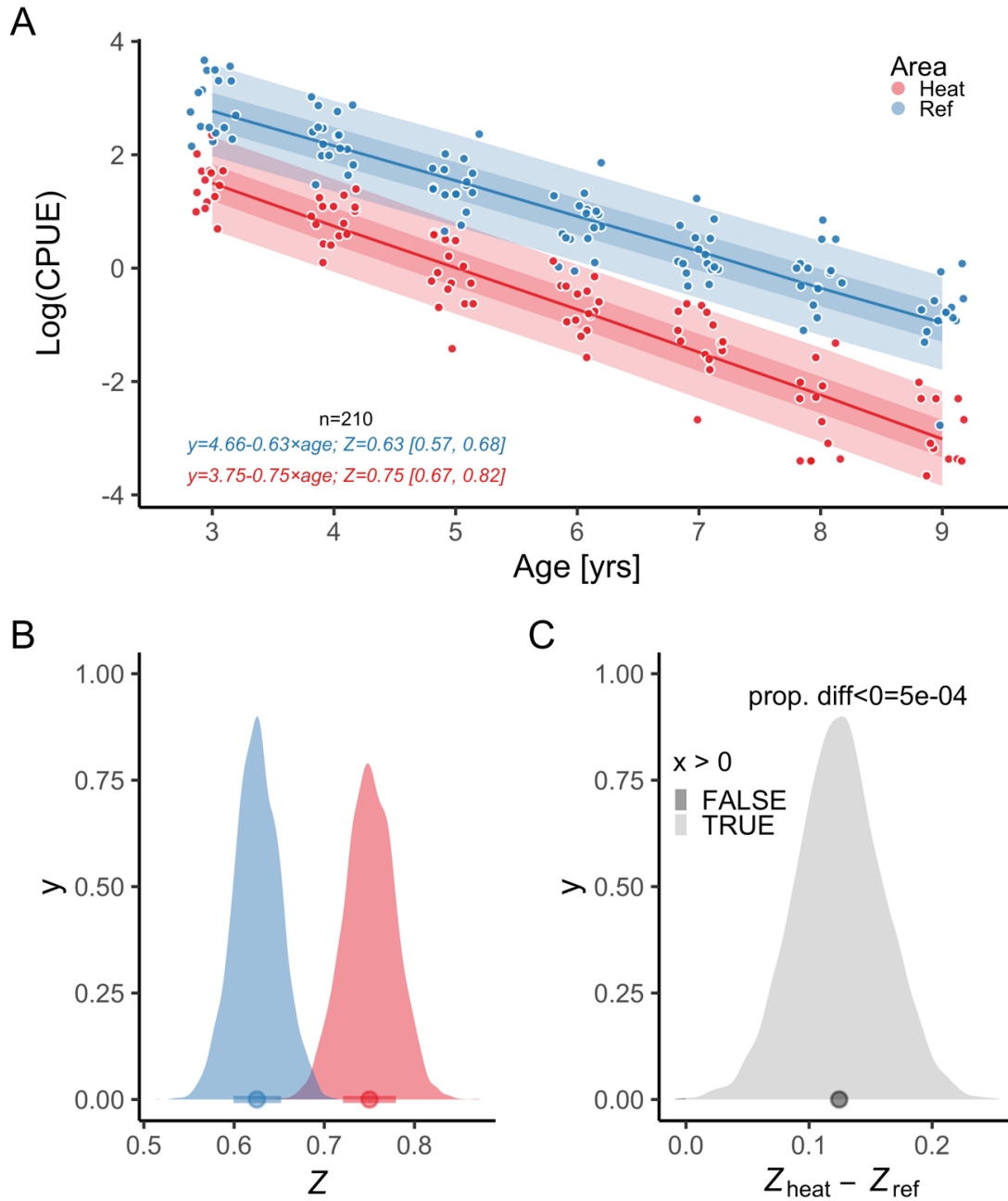


Fig. 4. The instantaneous mortality rate (Z) is higher in the heated area (red) than in the reference (blue). Panel (A) shows the $\log(\text{CPUE})$ as a function of age , where the slope corresponds to the global $-Z$. Lines show the posterior prediction without group-level effects (i.e., cohort) and the shaded areas correspond to the 50% and 90% credible intervals. The equation uses mean parameter estimates. Panel (B) shows the posterior distributions for mortality rate (Z_{heat} and Z_{ref}), and (C) the distribution of their difference.

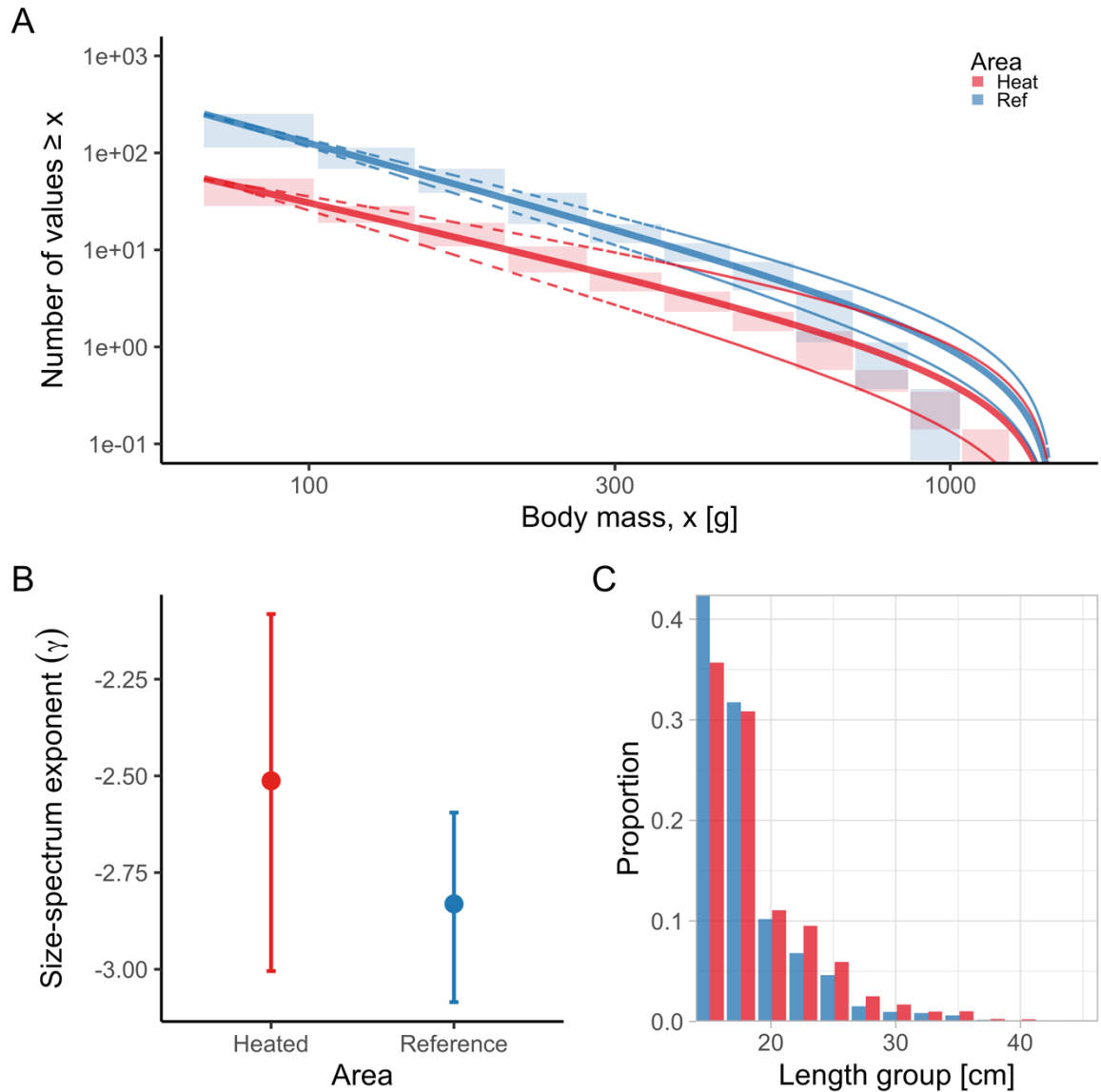


Fig. 5. The heated area (red) has a larger proportion of large fish than the reference area (blue), illustrated both in terms of the biomass size-spectrum (A), and histograms of proportions (C), but the difference in the slope of the size-spectra between the areas is not statistically clear (B). Panel (A) shows the size distribution and MLEbins fit (red and blue solid curve for the heated and reference area, respectively) with 95% confidence intervals indicated by dashed lines. The vertical span of rectangles illustrates the possible range of the number of individuals with body mass \geq the body mass of individuals in that bin. Panel (B) shows the estimate of the size-spectrum exponent, γ , and vertical lines depict the 95% confidence interval. Panel (C) illustrates histograms of length groups in the heated and reference area as proportions (for all years pooled).